

Finite Element Analysis of Stent Implantation in a Three-Dimensional Reconstructed Arterial Segment

Georgia S. Karanasiou, Claire Conway, Michail I. Papafaklis, Augusto C. Lopes, Kostas A. Stefanou, Lambros S. Athanasiou, Lampros K. Michalis, Elazer R. Edelman, Dimitrios I. Fotiadis, *Senior Member, IEEE*

Abstract—Endovascular stent deployment is a mechanical procedure used to rehabilitate a diseased arterial segment by restoring blood flow in occluded regions. The success or failure of the stent implantation depends on the stent device and the deployment technique. The optimal stent deployment can be predicted by investigating the factors that influence this minimally invasive procedure. In this study, we propose a methodology which evaluates the alterations in the arterial environment caused by stent deployment. A finite element model of a reconstructed right coronary artery with a stenosis was created based on anatomical information provided by intravascular ultrasound and angiography. The model was used to consider placement and performance after intervention with a commercially available Leader Plus stent. The performance of the stent, within this patient-specific arterial segment is presented, as well as the induced arterial deformation and straightening. The arterial stress distribution is analyzed with respect to possible regions of arterial injury. Our approach can be used to optimize stent deployment and to provide cardiologists with a valuable tool to visually select the position and deploy stents in patient-specific reconstructed arterial segments, thereby enabling new methods for optimal cardiovascular stent positioning.

I. INTRODUCTION

Cardiovascular disease (CVD), one of the most prevalent health problems, is the leading cause of mortality around the world [1]. CAD is caused by atherosclerosis, an accumulation of fatty deposits, called atherosclerotic plaques, underneath the endothelium which result in the disruption of the arterial structure and function [2]. The atherosclerotic plaques vary in composition (cholesterol, calcium and other lipids), morphology and pathophysiology. As atherosclerosis progresses, the arterial wall becomes more thick and stiff, while blood flow in coronary arteries is obstructed [3]. This

G.S. Karanasiou, K.A. Stefanou, and L.S. Athanasiou, are with the University of Ioannina, Department of Materials Science, Unit of Medical Technology and Intelligent Information Systems, Ioannina, Greece (e-mail: g.karanasiou@gmail.com, kstefan@cc.uoi.gr, lmathanas@cc.uoi.gr).

M.I. Papafaklis is with the Michailideion Cardiac Center, University of Ioannina, Ioannina, Greece (e-mail: m.papafaklis@yahoo.com).

C. Conway, A.C. Lopes and E.R. Edelman are with the Institute for Medical Engineering and Science, Massachusetts Institute of Technology, Cambridge, MA and Cardiovascular Division, Brigham and Women's Hospital USA (e-mail: cconway@mit.edu, aclopes@mit.edu, ere@mit.edu).

L.K. Michalis is with the Department of Cardiology, Medical School, University of Ioannina, Ioannina, Greece (e-mail: lmichalis@cc.uoi.gr).

D.I. Fotiadis is with the University of Ioannina, Department of Materials Science, Unit of Medical Technology and Intelligent Information Systems and with the Foundation for Research and Technology-Hellas (FORTH) Ioannina, Greece (e-mail: fotiadis@cc.uoi.gr).

may result in chest pain, heart attack or, in more severe cases, death [4].

CAD manifestations vary in time, space and individual patients, making it difficult to predict to whom and where lesions form and destabilize. It is well understood that genetic predisposition plays a crucial role to the set-up of this disease [5] and that the development and evolution of this disease are influenced by other factors such as obesity, smoking, high levels of cholesterol and high blood pressure [6], [7]. These pathologies have been traditionally modulated and treated through drug therapies [8]. Innovation on lifestyle modification and drug development has changed the treatment of CAD and yet there is a limit to what they can provide often requiring mechanical intervention. In high risk patients, more invasive treatment is preferred, such as arterial by-pass or PCI (Percutaneous Coronary Intervention). Coronary artery bypass grafting (CABG), the so-called artery bypass for CAD patients, is based on arterial or vein conduits (grafts) to bypass the occluded region of the artery, thus restoring blood flow [9]. PCI uses a balloon-catheter and through its inflation, the arterial wall is expanded, the arterial lumen is dilated and blood flow is restored. Once the balloon has fulfilled its purpose, it is removed, minimizing retained hardware but also in some cases enabling the artery to recoil elastically and return to its initial shape. Stenting, a combination of angioplasty and stent deployment, has been introduced to reduce restenosis. The stent, a tubular wire mesh which is inserted, inflated in the stenotic region and permanently left in place prevents arterial recoil and reclosure [10].

Stents have improved clinical outcomes in CAD treatment, but are beset by issues of their own – some related to the artery and others to the device itself. The local arterial injury induced by the stent may lead to tissue overgrowth and in-stent restenosis (ISR), while it also poses a risk for stent thrombosis (ST). The stent itself is subject to stresses and can fracture further exacerbating propensity for ISR and ST [11].

Computational simulations, based on the Finite Element Analysis (FEA), have attracted the interest of researchers in a range of fields and are especially valuable in dissecting out mechanisms of complex phenomena that can only be appreciated in a limited sector of the empirical domain. Computational methods have proved to be an excellent and effective tool for analyzing the mechanical performance of stents and investigating the arterial implications associated with stents of different designs and materials that cannot be fully evaluated in bench or animal experiments [12]–[14]. The mechanical behavior of the stent inside the diseased artery has been previously investigated considering the

arterial segment and the atherosclerotic plaque as idealized straight or curved cylinders [15]–[17]. Different stent deployment techniques have also been considered [18]. Different approaches can be considered using FEA including displacement driven paradigms where the stent is deployed by imposing a radial displacement in the inner surface of the stent, or pressure-driven modes where an inflation pressure is used for the stent deployment [19]. In some studies the balloon component is taken into consideration [20], [21], and in others the atherosclerotic plaque composition is included in the region of stenosis [22].

In the present study, we studied the expansion performance of the Leader Plus stent in a realistic reconstructed patient-specific right coronary arterial segment. Resultant stresses in the stent-arterial contact region were analyzed and correlated to the inflation pressure.

II. MATERIALS AND METHODS

A. 3D reconstruction

In order to reconstruct the three-dimensional (3D) right coronary artery, angiographic data and intravascular ultrasound (IVUS) images were obtained from a patient, affected by arterial hypertension and presenting elevated cholesterol levels (Fig. 1). The 3D artery reconstruction was performed using a previously validated methodology [23]. The lumen and media adventitia borders of the artery were detected and placed on the 3D lumen centerline. The two point clouds extracted represent the arterial wall and lumen anatomy. The reconstructed 3D arterial model was used for the structural analysis of the stent deployment procedure.

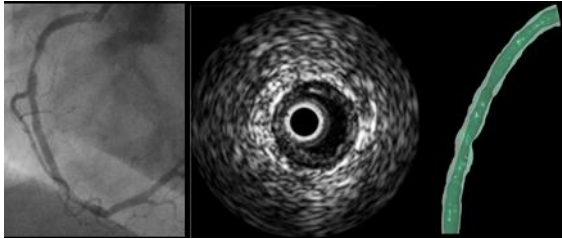


Figure 1. IVUS, angiography medical data and the reconstructed arterial segment.

B. Computational Simulation

The three-dimensional (3D) finite element model, required for the structural computational analysis, was generated in its unexpanded configuration and consisted of the 3D reconstructed arterial segment and the 3D stent design. Based on the Finite Element Method (FEM), ANSYS 14.5 (Ansys Canonsburg, PA) was used for the development of the model and for the post processing of the results [24]. The Leader Plus commercially available stent has an outer diameter of 1.42 mm and inner diameter of 1.26 mm and consists of 8 connected rings. The length of the reconstructed arterial segment is approximately 47mm (Fig. 2).

For the mesh generation, a 3D higher order 10 node element was selected. A mesh sensitivity analysis was performed, defining as a convergence criterion, the convergence of the maximum von Mises stresses being within 5%. There are many different modeling approaches

concerning the stent deployment simulation. In this study, we modeled stent expansion by imposing pressure directly on the nodes of the inner surface of the stent.

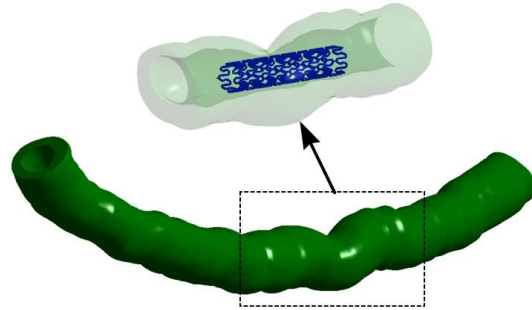


Figure 2. The reconstructed arterial segment and the finite element model pre simulation.

C. Material properties

Several material models can be used to represent the biomechanical behavior of the human tissue during the stent deployment. The artery was considered as homogenous, presenting a nonlinear behavior. The Mooney-Rivlin hyperelastic material model was selected for the arterial segment, defined by a polynomial form [25]. The strain energy density function W , in terms of the strain invariants (I_1, I_2, I_3) for this hyperelastic material, was described by Maurel *et al.* [26]:

$$W(I_1, I_2, I_3) = \sum_{p,q,r=0}^n C_{pqr} (I_1 - 3)^p (I_2 - 3)^q (I_3 - 3)^r, \quad (1)$$

where the strain invariants are defined as:

$$I_1 = \lambda_1^2 + \lambda_2^2 + \lambda_3^2, \quad (2)$$

$$I_2 = \lambda_1^2 \lambda_2^2 + \lambda_1^2 \lambda_3^2 + \lambda_2^2 \lambda_3^2, \quad (3)$$

$$I_3 = \lambda_1^2 \lambda_2^2 \lambda_3^2. \quad (4)$$

C_{pqr} is the hyperelastic constants, $C_{000} = 0$, and $\lambda_1, \lambda_2, \lambda_3$ are the principal stretches of the arterial wall.

More specifically, for the needs of this study, a third order five parameter specific form of (1) was selected (Table I) described by Eshghi *et al.* [27] as it is shown below:

$$W = C_{10} (I_1 - 3) + C_{01} (I_2 - 3) + C_{20} (I_1 - 3)^2 + C_{11} (I_1 - 3)(I_2 - 3) + C_{30} (I_1 - 3)^3, \quad (5)$$

A bi-linear elasto-plastic material model was employed for the stent with Elastic Modulus 232 GPa, Tangent Modulus 0.738 GPa and Poisson's ratio 0.32.

TABLE I. ARTERIAL WALL PROPERTIES

Arterial Material Properties	Arterial hyperelastic coefficients				
	C_{10}	C_{01}	C_{20}	C_{11}	C_{30}
	0.0189	0.00275	0.08572	0.5904	0

D. Boundary conditions

The stent was initially positioned in the region of the arterial stenosis. The artery was tethered at its ends to avoid any displacement or rotation. Appropriate boundary conditions were imposed to the stent nodes, allowing movement in the axial and radial directions. The stent expansion was achieved by enforcing a pressure of 1.5MPa on the nodes of the inner surface of the stent. The artery-stent contact pair was assumed to have a frictionless contact. Attention was paid in defining the analysis parameters, such as time step and surface to surface contact algorithm, to cope with large displacement difficulties and nonlinear contact problems. The Newton-Raphson's method was used to solve this non-linear problem.

III. RESULTS AND DISCUSSION

As stents are expanded under uniform pressure load, stent struts should deform uniformly. Arterial segments, however, tend not to be symmetrically stenosed and the deformed shape of the stent alters commensurate with lesion morphology (Fig 3). The response of the stent is of much importance as regions subject to high stresses increase the possibility of stent fracture, which in turn cause arterial injury, ISR and ST. FEA showed that the stent connectors are subject to higher local stresses, approaching 550 MPa, as these areas are subject to plastic deformation.

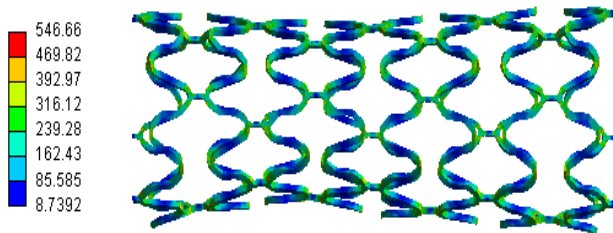


Figure 3. Stress distribution (MPa) on the expanded stent.

To better understand the mechanical performance of the stent, the expanded radius against the expanding pressure was evaluated, for three symmetrical points, located in the inner middle cross section of the stent (Fig. 4).

We observed that the rate of increment of the stent radius was not proportional to the inflation pressure. The stent radius increased slowly at inflations pressure lower than 0.75 MPa and far more rapidly and significantly thereafter - plateauing at 1.16 mm at 1.5 MPa.

The von Mises stresses in the arterial wall during the stent deployment and more specifically for the inflation pressures of 1.2-1.5 MPa (Fig. 5) caused alterations in the shape of the arterial wall. Higher von Mises stresses were delivered in the contact area of stent-arterial wall as inflation rises and especially in areas of stenosis. The risk of arterial damage rises with higher stresses even if blood flow is restored. The eccentricity in lesion morphology leads to asymmetric distribution of the von Mises stress (Fig. 6). In the area of stenosis, across the arterial thickness, the stress decreased as the distance from the inner arterial surface increased.

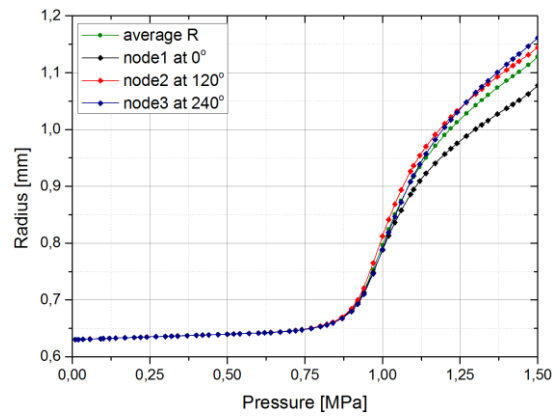


Figure 4. The relation between the expanding pressure with three symmetrical points, located in the inner middle cross-section of the stent.

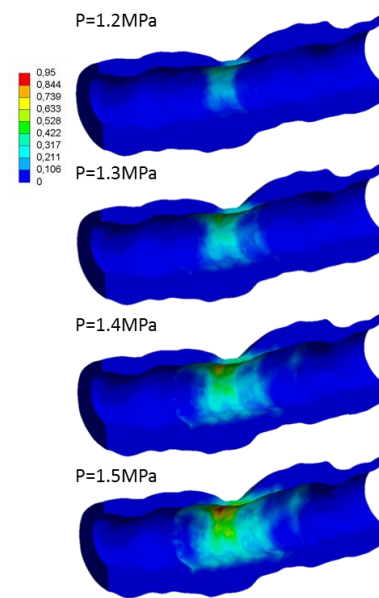


Figure 5. Arterial von Mises stress (MPa) during stent expansion.

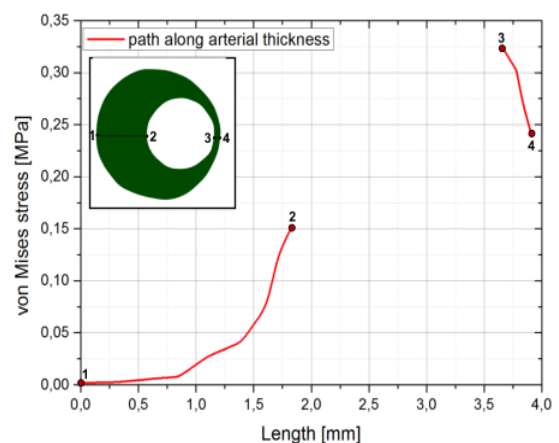


Figure 6. Von Mises stress distribution for two selected paths in the middle arterial stenosis cross section.

In detail, the stress at point 1 was negligible whereas the stress at point 2 was approximately 0.15MPa. Additionally, comparing the stresses observed along these two paths, it was demonstrated that the stress increases as the arterial thickness decreases.

IV. CONCLUSIONS

FEA explained how deployment of a commercially available stent can minimize arterial injury and potential complications. This approach could assist cardiologists in visualizing and evaluating stent deployment by selecting different stent designs and imposing the optimal inflation pressure in patient-specific arterial segments.

One main limitation of the work is the lack of validating our computational results. Another assumption is that the arterial wall was modeled as an isotropic, homogenous and hyperelastic material.

In the future, we will use pre and post-stenting medical data of patient-specific arterial segments aiming to validate our model.

ACKNOWLEDGMENT

The authors thank the Rontis Medical Device Company [28] for providing all the necessary information regarding their stent devices. Elazer R. Edelman is supported in part by a grant from the US National Institutes of Health (GM R01 49039).

REFERENCES

- [1] "WHO | Cardiovascular diseases (CVDs)," *WHO*. [Online]. Available: <http://www.who.int/mediacentre/factsheets/fs317/en/>. [Accessed: 08-Mar-2014].
- [2] B.-H. Toh, T. Kyaw, P. Tipping, and A. Bobik, "Chapter 71 - Atherosclerosis," in *The Autoimmune Diseases (Fifth Edition)*, N. R. Rose and I. R. Mackay, Eds. Boston: Academic Press, 2014, pp. 1049–1066.
- [3] A. Kumar, "Computational Model of Blood Flow in the Presence of Atherosclerosis," in *6th World Congress of Biomechanics (WCB 2010). August 1-6, 2010 Singapore*, C. T. Lim and J. C. H. Goh, Eds. Springer Berlin Heidelberg, 2010, pp. 1591–1594.
- [4] L. Badimon, T. Padró, and G. Vilahur, "Atherosclerosis, platelets and thrombosis in acute ischaemic heart disease," *Eur. Heart J. Acute Cardiovasc. Care*, vol. 1, no. 1, pp. 60–74, Apr. 2012.
- [5] N. Yiannakouris, M. Katsoulis, V. Dilis, L. D. Parnell, D. Trichopoulos, J. M. Ordovas, and A. Trichopoulou, "Genetic predisposition to coronary heart disease and stroke using an additive genetic risk score: A population-based study in Greece," *Atherosclerosis*, vol. 222, no. 1, pp. 175–179, 2012.
- [6] L. Djoussé, J. A. Driver, and J. Gaziano, "Relation between modifiable lifestyle factors and lifetime risk of heart failure," *JAMA*, vol. 302, no. 4, pp. 394–400, 2009.
- [7] A. R. Folsom, K. Yamagishi, A. Hozawa, L. E. Chambless, and Atherosclerosis Risk in Communities Study Investigators, "Absolute and attributable risks of heart failure incidence in relation to optimal risk factors," *Circ. Heart Fail.*, vol. 2, no. 1, pp. 11–17, Jan. 2009.
- [8] H. Nakamura, K. Arakawa, H. Itakura, A. Kitabatake, Y. Goto, T. Toyota, N. Nakaya, S. Nishimoto, M. Muranaka, A. Yamamoto, K. Mizuno, Y. Ohashi, and MEGA Study Group, "Primary prevention of cardiovascular disease with pravastatin in Japan (MEGA Study): a prospective randomised controlled trial," *Lancet*, vol. 368, no. 9542, pp. 1155–1163, Sep. 2006.
- [9] L. D. Cornwell, O. Preventza, and F. Bakaeen, "Chapter 21 - Coronary Artery Bypass Surgery," in *Cardiology Secrets (Fourth Edition)*, G. N. Levine, Ed. Philadelphia: W.B. Saunders, 2014, pp. 158–165.
- [10] A. M. Joyce and G. G. Ginsberg, "Chapter 17 - Expandable Stent Insertion," in *ERCP*, T. H. Baron, R. Kozarek, and D. L. Carr-Locke, Eds. Edinburgh: W.B. Saunders, 2008, pp. 165–176.
- [11] D. Surdell, A. Shaibani, B. Bendok, and M. K. Eskandari, "Fracture of a nitinol carotid artery stent that caused restenosis," *J. Vasc. Interv. Radiol. JVIR*, vol. 18, no. 10, pp. 1297–1299, Oct. 2007.
- [12] M. Azaouzi, A. Makradi, J. Petit, S. Belouettar, and O. Polit, "On the numerical investigation of cardiovascular balloon-expandable stent using finite element method," *Comput. Mater. Sci.*, vol. 79, pp. 326–335, 2013.
- [13] M. Azaouzi, A. Makradi, and S. Belouettar, "Numerical investigations of the structural behavior of a balloon expandable stent design using finite element method," *Comput. Mater. Sci.*, vol. 72, pp. 54–61, 2013.
- [14] Z. P. W. Walke, "Experimental and numerical biomechanical analysis of vascular stent," *J. Mater. Process. Technol. - JMATER PROCESS TECHNOL*, vol. 164, pp. 1263–1268, 2005.
- [15] S. N. David Chua, B. J. MacDonald, and M. S. J. Hashmi, "Finite element simulation of slotted tube (stent) with the presence of plaque and artery by balloon expansion," *J. Mater. Process. Technol.*, vol. 155–156, pp. 1772–1779, Nov. 2004.
- [16] S. Zhao, L. Gu, S. R. Froemming, J. M. Hammel, and H. Lang, "Finite Element Analysis of Stent Deployment in a Stenotic Artery and Their Interactions," in *(iCBBE) 2011 5th International Conference on Bioinformatics and Biomedical Engineering*, 2011, pp. 1–4.
- [17] W. Wu, W.-Q. Wang, D.-Z. Yang, and M. Qi, "Stent expansion in curved vessel and their interactions: a finite element analysis," *J. Biomech.*, vol. 40, no. 11, pp. 2580–2585, 2007.
- [18] F. Gervaso, C. Capelli, L. Petrini, S. Lattanzio, L. Di Virgilio, and F. Migliavacca, "On the effects of different strategies in modelling balloon-expandable stenting by means of finite element method," *J. Biomech.*, vol. 41, no. 6, pp. 1206–1212, 2008.
- [19] G. S. Karanasiou, A. I. Sakellarios, E. E. Tripoliti, E. G. M. Petrakis, M. E. Zervakis, F. Migliavacca, G. Dubini, E. Dordoni, L. K. Michalis, and D. I. Fotiadis, "Modeling of Stent Implantation in a Human Stenotic Artery," in *XIII Mediterranean Conference on Medical and Biological Engineering and Computing 2013*, L. M. R. Romero, Ed. Springer International Publishing, 2014, pp. 1045–1048.
- [20] T. C. Gasser and G. A. Holzzapfel, "Finite Element Modeling of Balloon Angioplasty by Considering Overstretch of Remnant Non-diseased Tissues in Lesions," *Comput. Mech.*, vol. 40, no. 1, pp. 47–60, Jun. 2007.
- [21] F. Ju, Z. Xia, and K. Sasaki, "On the finite element modelling of balloon-expandable stents," *J. Mech. Behav. Biomed. Mater.*, vol. 1, no. 1, pp. 86–95, Jan. 2008.
- [22] K. Takashima, T. Kitou, K. Mori, and K. Ikeuchi, "Simulation and experimental observation of contact conditions between stents and artery models," *Med. Eng. Phys.*, vol. 29, no. 3, pp. 326–335, Apr. 2007.
- [23] C. V. Bourantas, M. I. Papafaklis, L. Athanasiou, F. G. Kalatzis, K. K. Naka, P. K. Siogkas, S. Takahashi, S. Saito, D. I. Fotiadis, C. L. Feldman, P. H. Stone, and L. K. Michalis, "A new methodology for accurate 3-dimensional coronary artery reconstruction using routine intravascular ultrasound and angiographic data: implications for widespread assessment of endothelial shear stress in humans," *EuroIntervention J. Eur. Collab. Work. Group Interv. Cardiol. Eur. Soc. Cardiol.*, vol. 9, no. 5, pp. 582–593, Sep. 2013.
- [24] "Ansys Mechanical." [Online]. Available: <http://www.ansys.com>.
- [25] C. Lally, A. J. Reid, and P. J. Prendergast, "Elastic behavior of porcine coronary artery tissue under uniaxial and equibiaxial tension," *Ann. Biomed. Eng.*, vol. 32, no. 10, pp. 1355–1364, Oct. 2004.
- [26] D. Thalmann, Y. Wu, N. M. Thalmann, and W. Maurel, *Biomechanical Models for Soft Tissue Simulation*, vol. XVIII. 1998.
- [27] N. Eshghi, M. H. Hojjati, M. Imani, and A. M. Goudarzi, "Finite Element Analysis of Mechanical Behaviors of Coronary Stent," *Procedia Eng.*, vol. 10, pp. 3056–3061, 2011.
- [28] "Rontis Medical Device Co." [Online]. Available: <http://www.rontis-ag.com/>.